JACS
JOURNAL OF THE AMERICAN CHEMICAL SOCIETY

Communication

pubs.acs.org/JACS

Complementary Helicity Interchange of Optically Switchable Supramolecular-Enantiomeric Helicenes with (−)-Gel-Sol-(+)-Gel Transition Ternary Logic

Chien-Tien Chen,*[,†] Chien-Hsiang Chen,[‡] and Tiow-Gan Ong[§]

[†]Department of Chemistry, National Tsing-Hua University, Hsinchu, Taiwan

[‡]National Taiwan Normal University, Taipei, Taiwan

[§]Institute of Chemistry, Academia Sinica, Taipei, Taiwan

Supporting Information

ABSTRACT: A gallamide-containing pseudoenantiomeric helicene pair bearing a (10*R*,11*R*)-dimethoxymethyldibenzosuberane core can self-assemble by intermolecular amide H-bonding and π-π stacking into bundled helical fibers with helical tunnels of complementary helicity in CH_2Cl_2. The helicenes undergo excellent complementary photoswitchings of ternary logic at 280, 318, and 343 nm through (−)-gel-sol-(+)-gel interconversion.

Transmission of chiral information from molecular to macro- or even supramolecular levels[1] (i.e., asymmetric transcription) is a powerful mechanism adopted in nature for the controlled self-assembly of chiral subunits into complex superstructures with well-defined functions due to unique 3-D molecular shapes and cavities. Helical domain(s) in macromolecules such as starch, protein, and DNA may thus be generated.[2] H-bonding, electrostatic, π-π, and van der Waals (vdW) interactions are the major molecular forces involved in triggering these self-assembly processes. As inspired by nature, synthetic systems offer a diverse array of opportunities to control the properties of materials in a dynamic, modulable, and even reversible manner. By taking advantage of these molecular forces, one can also trigger the self-assembly of custom-designed small molecules into large polymer-like aggregates or gel networks. Low-molecular-weight gelators (LMWGs) are organic compounds with MW < 3000 Da[3] that can form gels in organic solvents and/or water at low concentrations (2−10 wt%).[4] Weak interactions like those mentioned above can lead to formation of a gel network.[5] The ordered arrangement in organogels made by physical interplay can be perturbed by forces including heat, light, chemical additives, and mechanical action. These factors facilitate control over the sol-to-gel interchange. Despite advances in the use of LMWGs in many applications,[6] chiral helical variants of LMWGs are relatively unexplored.[7a−d] To date, in situ direct helicity interchanges in helical organogels by external stimulators[7e] remain a challenge, even though helicity reversal in local segment(s) of gel fibers has been observed by thermal control[7f] or changes in gelator loading.[7g,h] Seminal work by Feringa et al. successfully addressed this issue using 1,2-thienylcyclopentene bearing chiral amide arms by temperature-modulated, light-triggered reversible transcription of macroscopic into molecular chirality.[7b,i,j] They also developed *N*-hexylurea-based helical polymers bearing a photoswitchable fluorene-based helicene head unit, allowing for efficient "sergeants and soldiers" and/or "majority rules" induced control of polymer helicity.[7g,8]

Scheme 1. Photoswitchable Helicene Gelator by Self-Assembly

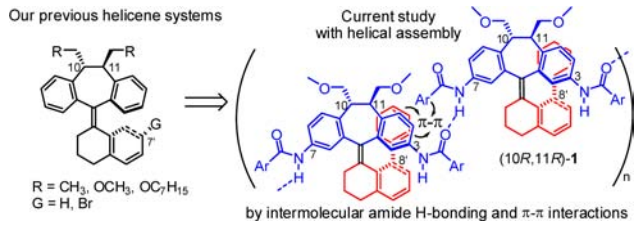

As part of our ongoing research on the uses of C_2-symmetric dibenzosuberane (DBS)-based helicenes as conformation-modulable, chirochromic optical switches having reversible, complementary helicities (*M* or *P*′) in liquid-crystalline materials,[9] we sought to evaluate the feasibility of their use for chiral organogel formation by the "sergeants and soldiers" or "majority rules" effect,[10c] with complementary helicity interchanges that are switchable by light.

In contrast to our previous molecular designs of photoswitchable helicenes, here we invoked a unique type of helicene, **1**, incorporating aromatic amide ("aramide") moieties at both the C3 and C7 positions in the top C_2-symmetric DBS template (Scheme 1). In addition to H-bonding and π-π interactions, extra vdW forces were introduced by appending long-chain alkyl groups at the 3, 4, and 5 positions of the aramides to effect interchain alignment, further facilitating organogel formation.[10] Furthermore, a phenyl ring was introduced at the C8′ position of the bottom tetralin template to enhance the π-π interactions (edge-to-edge distance = 3.33 Å) and thus the helical nature of the resulting organogels.[11]

To identify two different irradiation wavelengths to achieve photochemical switching between two pseudoenantiomeric helicenes with complementary helicities, their individual UV/vis and difference spectra with discernible extinction coefficient changes ($\Delta\varepsilon$) were measured, allowing their relative composition at the photostationary state (pss) of a given irradiation wavelength to be assessed. The diastereomeric excess at the pss

Received: February 3, 2013
Published: March 22, 2013

   dx.doi.org/10.1021/ja401214t | *J. Am. Chem. Soc.* 2013, 135, 5294−5297

Scheme 2. Photoisomerization Profiles of Helicenes (*M*)-1 and (*P*)-1′ in *n*-Hexane or CH_2Cl_2 (1×10^{-5} M)

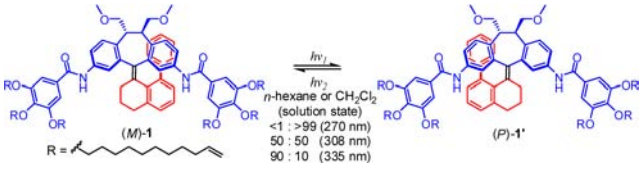

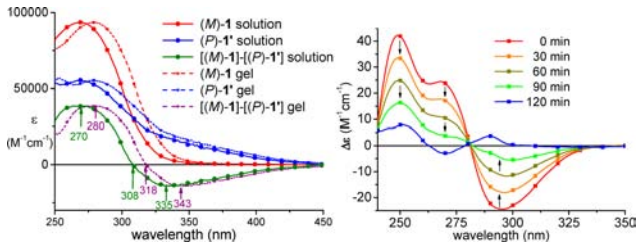

Figure 1. (left) UV/vis and difference spectra of (*M*)-**1** and (*P*)-**1′** in solution (*n*-hexane) and gel (CH_2Cl_2). (right) Stacked CD dynamic plots before and after irradiation of (*M*)-**1** (1.0×10^{-5} M) at 270±4 nm.

($[de]_{pss}$) at a given wavelength can often be directly determined by the difference in the extinction coefficients under the condition that the photoisomerization quantum yields for the two processes ($\Phi_{M\rightarrow P}$ and $\Phi_{P\rightarrow M}$) stay similar. Thus, to attain efficient photoswitching in a highly selective manner, it is better to focus the photoirradiation on regions with the largest complementary changes in the extinction coefficients.

Initial photoisomerization experiments were carried out by irradiating (10*R*,11*R*,*M*)-**1** [denoted as (*M*)-**1**] at 254 nm, as was done previously for helicenes bearing (10*R*,11*R*)-diethyl-[9a,b] and -dimethoxymethyl-substituted[9c] top templates. Notably, diastereomeric switching of (*M*)-**1** at 254 nm in *n*-hexane or CH_2Cl_2 led to exclusive formation of (*P*)-**1′** [(*M*)-**1**/(*P*)-**1′** = <1/>99, as determined by HPLC analysis of the reaction mixture (Scheme 2 and Figures S2 and S2′]. Subsequent photoisomerization experiments were performed at 270, 308, and 335 nm based on the UV/vis difference spectrum between (*M*)-**1** and (*P*)-**1′** (Figure 1 left). The detector wavelength for HPLC was set at 308 nm, the isosbestic point in the stacked UV/vis spectra of (*M*)-**1** and (*P*)-**1′** (Figure 1 left). Highly diastereoselective and complementary switching selectivities could thus be achieved upon photoirradiation of (*M*)-**1** at 270 nm [(*M*)-**1**/(*P*)-**1′** = <1/>99] and (*P*)-**1′** at 335 nm [(*M*)-**1**/(*P*)-**1**, 90/10] (Figures S2 and S2′). Notably, a pseudoracemic mixture [(*M*)-**1**/(*P*)-**1′** = 50/50] was obtained upon irradiation at 308 nm in *n*-hexane or CH_2Cl_2 (Scheme 2). In addition, split Cotton effects of complementary exciton chirality were observed in the circular dichroism (CD) spectra associated with the UV band at 280 nm for (*M*)-**1** and (*P*)-**1′** (Figure 1 right), attributed to the change in the electric transition dipole moment from the bottom 8′-phenyl template to the top-right benzamide-substituted phenyl ring. In contrast, only moderate diastereoselectivity (*M*/*P*′ = 25/75 at 280 nm) was observed for the helicene without the 8′-phenyl appendage. Thus, introduction of the 8′-phenyl moiety was essential to secure high switching profiles. Presumably, the intramolecular π-π interaction between the 8′-phenyl group and the DBS template can prevent undesired electrocyclization and also increase the thermal stability of the helical configuration.

Of seven different solvents tested for possible gel formation, (*M*)-**1** and (*P*)-**1′** remained dissolved in *n*-hexane, cyclohexane, benzene, and toluene even at 0.01 M at ambient temperature but

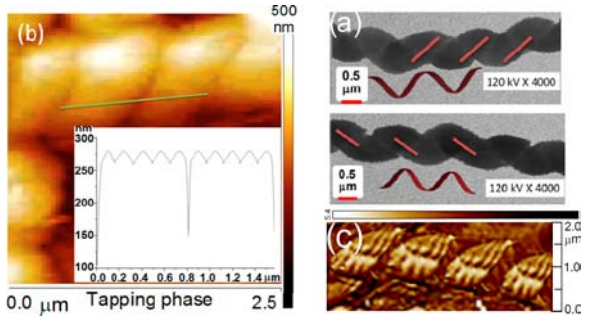

Figure 2. (a) TEM images of the bundled superstructures of xerogels from (top) (*M*)-**1** and (bottom) (*P*)-**1′**. (b) Tapping-mode AFM image of a sample obtained by spin-coating a solution of (*M*)-**1** in CH_2Cl_2. Inset: cross-section analysis along the green line. (c) AFM image of the same sample taken after 1 week.

formed gels in CH_2Cl_2, $CHCl_3$, and CH_3CN at a minimum concentration of 1×10^{-3} M (i.e., ≥2 mg/mL). The resulting gels were stable at ambient temperature, and the gel-to-sol interconversion was reversible upon repetitive heating (≥35 °C) and cooling cycles (Figure S3). Optimal concentrations for gelation in CH_2Cl_2 ranged from 2 to 20 mg/mL.

UV/vis, UV/vis difference, and CD spectra of (*M*)-**1**- and (*P*)-**1′**-doped CH_2Cl_2 gels were red-shifted by 10 nm relative to those taken in *n*-hexane solution (Figure 1 left and Figure S4), indicating their better π-π conjugation and/or stacking in the gel states. Dried organogels (i.e., xerogels) formed from (*M*)-**1**- and (*P*)-**1′**-doped CH_2Cl_2 gels showed left- and right-handed helical fibril rope morphologies, respectively, as confirmed by transmission electron microscopy (TEM) (Figures 2a and S5). For both, the helical pitch was 1.5−1.6 μm. The tapping-mode atomic force microscopy (AFM) image and cross-section profile of a sample prepared by spin-coating a 1.0 mM solution of (*M*)-**1** in CH_2Cl_2 onto highly ordered pyrolytic graphite shows four repetitive 20 nm deep minor grooves for each 130 nm deep major groove within a bundled fibril tube (Figures 2b and S7a). The distance between major grooves is 800 nm, and that between minor grooves is 160 nm. This indicates that a bundled fibril tube consists of five bundled fibers (Figure S6), as evidenced by the AFM image of the same sample taken after 1 week (Figures 2c and S7b). Thus, hierarchical self-assembly of the helicene monomers may be involved in formation of the bundled helical fibril tubes.[10e,k] Furthermore, a 105±5 nm diameter helical tunnel exists inside each bundled fibril tube.

Notably, (*M*)-**1** and (*P*)-**1′** helicenes led to the corresponding *M*- and *P*-form helical fibers. Thus, the absolute chirality of the helicene dictates the overall helical chirality of the self-assembled helical fibers, presumably through intermolecular H-bonding and π-π interactions.

FT-IR spectra of helicene (*M*)-**1** both in solution (1.0×10^{-5} M) and in gel (1.7×10^{-3} M) were also examined (Figure S8). In solution, the N−H and C═O stretching modes appeared at 3439 and 1806 cm^{-1}, respectively. After gel formation, these bands were shifted to lower energy (3283 and 1733 cm^{-1}, respectively), presumably because of facile intermolecular N−H···O═C H-bonding in the gel. The downfield shift of the N−H resonances of (*M*)-**1** from 7.62 to 8.73 ppm in concentration-dependent ^{1}H NMR experiments (0.4−1.1 mM range in CD_2Cl_2) confirmed the N−H···O═C H-bonding (Figure 3).

To gain insight into the critical composition(s) of (*M*)-**1**/(*P*)-**1′** in CH_2Cl_2 to maintain the gel state at the minimal dopant loading (i.e., 2−3 mg/mL or (1.2−1.7)$\times10^{-3}$ M), we performed

dx.doi.org/10.1021/ja401214t | J. Am. Chem. Soc. 2013, 135, 5294−5297

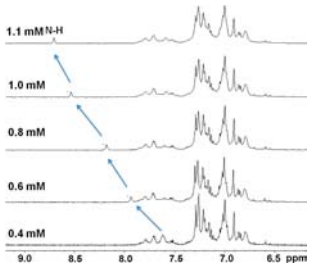

Figure 3. Expanded stacked ^{1}H NMR spectra of (*M*)-**1** at 0.4−1.1 mM in CD_2Cl_2 solution.

Figure 4. Photographs of the gel (3 mg/mL in CH_2Cl_2) at ambient temperature after irradiation of the original (*M*)-**1**-containing gel at 318 nm for at least 60 min (middle) and then at 280 nm (right) or 343 nm (left) for another 6−8 h.

the photoisomerization experiments using the gels at ambient temperature. Upon irradiation of pure (*M*)-**1**-containing gel in a sealed quartz cuvette (1 cm path length) at 318±4 nm with a monochromator light source, the gel turned into a homogeneous solution after 60 min, with the overall dopant composition reaching (*M*)-**1**/(*P*)-**1**′ = 60/40 (Figures 4 and S9). Further irradiation of the homogeneous solution at 280±4 nm for 60 min led to an overall dopant composition of 25/75, where the complementary helical gel state started to form, and the dopant composition gradually shifted to pure (*P*)-**1**′ after another 6 h of irradiation. Conversely, irradiation of the homogeneous solution [(*M*)-**1**/(*P*)-**1**′ = 50/50] at 343±4 nm led to a dopant composition of 69/31, in which the original gel state began to be restored, and the dopant composition gradually returned to the initial (*M*)-**1** state [(*M*)-**1**/(*P*)-**1**′ = 90/10] after another 8 h of irradiation. Thus, the helical superstructures of the bundled helical fibril tubes can be controlled in a complementary and reversible fashion by exposing the gel materials to either 280 or 343 nm irradiation.

Both UV/vis and CD/optical rotatory dispersion (ORD) dynamic tracing experiments were carried out to gain insight into the (−)-gel-sol-(+)-gel transition profiles. The UV λ_{max} at 280 nm was completely shifted to 270 nm when the overall composition of (*M*)-**1**/(*P*)-**1**′ in CH_2Cl_2 was changed from 70/30 to 60/40 (Figure S10), where the initial (−)-gel completely turned into the sol. Conversely, the CD null point at 291 nm, associated with the negative exciton chirality of the bundled (−)-helical fibers, was completely shifted to 280 nm (Figure 5).

In addition, the negative Cotton effect peak at 306 nm was completely shifted to 296 nm. The sol remained unchanged until the overall composition reached (*M*)-**1**/(*P*)-**1**′ ≈ 30/70, where the UV λ_{max} at 270 nm changed back to 280 nm and the sol started turning into the complementary (+)-gel state. In the meantime, an inverted CD/ORD peak at 300 nm started to appear and then ultimately displayed a positive Cotton effect at 300 nm as well as a positive exciton chirality in the pure (*P*)-**1**′ gel with the null point back to 291 nm. Photostabilities of both (*M*)-**1** and (*P*)-**1**′ in the warm gel states were monitored by UV/vis

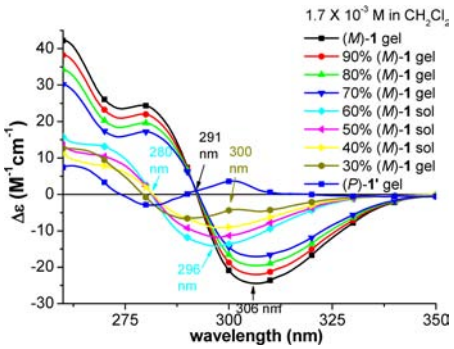

Figure 5. Expanded stacked CD/ORD plots of the photoisomerization tracing experiments on the (*M*)-**1** gel.

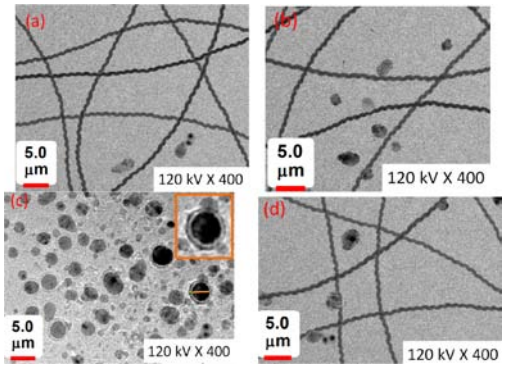

Figure 6. TEM images of bundled xerogel superstructures with the overall (*M*)-**1**/(*P*)-**1**′ composition (1.7×10^{-3} M in CH_2Cl_2) changed from 100/0 to (a) 90/10, (b) 70/30, (c) 50/50 (inset: expanded image), and (d) 20/80.

and CD/ORD throughout the photoswitching experiments and found to remain intact for five consecutive cycles (Figure S11).

Two possible pathways can account for photoswitching in gel−sol transitions. One involves local helical chirality switching that subsequently induces the neighboring helicenes to switch synergistically in the assembled single or bundled fibers. The other involves initial detachment of the photoisomerized helicenes or single fibers from the original homochiral bundled fibers and subsequent reassembly of the freely dissociated helicenes or single fibers of the same chirality to form the supramolecular enantiomeric bundled fibers.

In a series of TEM images taken from these photoisomerization experiments, only either pure (*M*)- or (*P*)-form bundled fibril tubes were observed when the overall composition ranged from (*M*)-**1**/(*P*)-**1**′ = >99/<1 to 70/30 and 25/75 to <1/>99, respectively (Figure 6; see Figure S12 for larger images). Notably, increasing amounts of micelles or vesicles were observed for the intermediate gel and sol states. In particular, only micelles or vesicles (~3.3 μm i.d., 0.52 μm thick) were observed at 50/50 overall composition even though the helicenes were still engaged in intermolecular H-bonding, as evidenced by the IR spectrum in CH_2Cl_2 (Figure S8). Two different sets of N−H and C═O stretching modes were observed, indicating formation of both homochiral and heterochiral aggregates.

The results suggest that photoisomerization in the gel may proceed through the second mechanism, where initially detached pseudoenantiomeric helicenes or single fibers from the original homochiral bundled fibers get dissolved and confined in CH_2Cl_2. They then gradually reassemble to form the complementary bundled fibers, subsequently furnishing the complementary

dx.doi.org/10.1021/ja401214t | J. Am. Chem. Soc. 2013, 135, 5294−5297

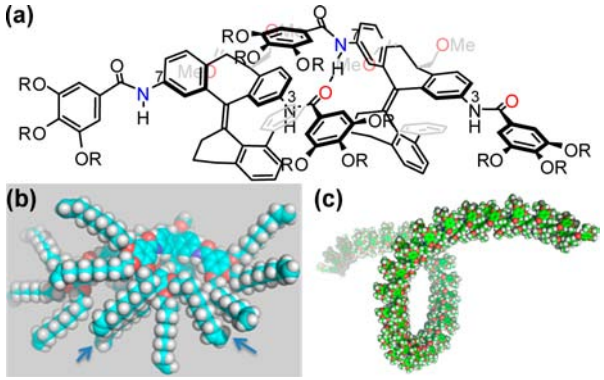

Figure 7. (a) Proposed mode of amide H-bonding in the dimer of (*M*)-**1**. (b) Proposed mode of vdW-induced alignments, shown as a CPK model. (c) Side view of the simulated left-handed helical assembly of the (*M*)-**1**-based 32-mer (R = CH_3 for simplicity).

bundled gel state once the minimal gelation concentration is reached. Since no local twisting or unfolding of fragments in bundled fibers was observed in the TEM images, synergistic photoisomerization within the single fibers is also possible.

The mechanism of helical fiber and subsequent bundle formation may have to do with facilitating self-assembly by repetitive intermolecular amide H-bonding, π-π, and vdW interactions. Preliminary molecular simulations of (*M*)-**1** dimer assembly with these three implemented forces in a ladder-type fashion indicated the involvement of facile H-bonding (~2.00 Å) between the C7 amido N−H and the C3 amido C═O units as the H-bond donor and acceptor (Figure 7a), respectively. Under such circumstances, each gallamide moiety exhibits two pairs of favorable vdW-induced alignments[10] between the meta-substituted dodec-1-enyloxy groups (Figure 7b). Further extensive optimizations of these key interactions in a repetitive ladder assembly for a 32-mer clearly led to the expected left-handed helical assembly with a helical pitch of ~250 nm (Figure 7c).

■ ASSOCIATED CONTENT

Supporting Information

Experimental details and additional data. This material is available free of charge via the Internet at http://pubs.acs.org.

■ AUTHOR INFORMATION

Corresponding Author

ctchen@mx.nthu.edu.tw

Notes

The authors declare no competing financial interest.

■ ACKNOWLEDGMENTS

We thank the National Science Council of Taiwan for financial support of this research (98-2119-M-007-012-MY3). Dedicated to Prof. Scott E. Denmark on the occasion of his 60th birthday.

■ REFERENCES

(1) Feringa, B. L.; Van Delden, R. A. *Angew. Chem., Int. Ed.* **1999**, *38*, 3418.

(2) (a) Schulz, G. E.; Schirmer, R. H. *Principles of Protein Structure*; Springer: New York, 1979. (b) Saenger, W. *Principles of Nucleic Acid Structure*; Springer: New York, 1984.

(3) Weiss, R. G.; David, J. A. *Adv. Mater.* **2000**, *12*, 1237.

(4) (a) Terech, P.; Weiss, R. G. *Chem. Rev.* **1997**, *97*, 3133. (b) Gronwald, O.; Shinkai, S. *Chem.—Eur. J.* **2001**, *7*, 4328. (c) Van Esch, J. H.; Feringa, B. L. *Angew. Chem., Int. Ed.* **2000**, *39*, 2263.

(5) (a) Lin, Y.; Kachar, B.; Weiss, R. G. *J. Am. Chem. Soc.* **1989**, *111*, 5542. (b) Fenniri, H.; Mathivanan, P.; Vidale, K. L.; Sherman, D. M.; Hallenga, K.; Wood, K. V.; Stowell, J. G. *J. Am. Chem. Soc.* **2001**, *123*, 3854.

(6) Chemical and fluorescent sensing: (a) Nakayama, D.; Takeoka, Y.; Watanabe, M.; Kataoka, K. *Angew. Chem., Int. Ed.* **2003**, *42*, 4197. (b) Cicchi, S.; Pescitelli, G.; Lascialfari, L.; Ghini, G.; di Bari, L.; Brandi, A.; Bussotti, L.; Atsbeha, T.; Marcelli, A.; Foggi, P.; Berti, D.; Mannini, M. *Chirality* **2011**, *23*, 833. Drug delivery: (c) Tiller, J. C. *Angew. Chem., Int. Ed.* **2003**, *42*, 3072. Tissue engineering: (d) Abdallah, D. J.; Weiss, R. G. *Adv. Mater.* **2000**, *12*, 1237. Cosmetics: (e) Haering, G.; Luisi, P. L. *J. Phys. Chem.* **1986**, *90*, 5892. Controlled release: (f) Karinaga, R.; Jeong, Y.; Shinkai, S.; Kaneko, K.; Sakurai, K. *Langmuir* **2005**, *21*, 9398. Catalysis and template materials: (g) Gao, P.; Zhan, C. L.; Liu, M. H. *Langmuir* **2006**, *22*, 775. (h) Van Bommel, K. J. C.; Friggeri, A.; Shinkai, S. *Angew. Chem., Int. Ed.* **2003**, *42*, 980. (i) Kim, S. S.; Zhang, C. P. *Science* **1998**, *282*, 1302. (j) Jung, J. H.; Ono, Y.; Hanabusa, K.; Shinkai, S. *J. Am. Chem. Soc.* **2000**, *122*, 5008. Pollutant capture: (k) Kiyonaka, S.; Sugiyasu, K.; Shinkai, S.; Hamachi, I. *J. Am. Chem. Soc.* **2002**, *124*, 10954. Chiral adsorbents: (l) Kobayashi, A.; Hamasaki, N.; Suzuki, M.; Kimura, M.; Shirai, H.; Hanabusa, K. *J. Am. Chem. Soc.* **2002**, *124*, 6550. (m) Jung, H. J.; Ono, Y.; Shinkai, S. *Angew. Chem., Int. Ed.* **2000**, *39*, 1862. A recent review: (n) Dawn, A.; Shiraki, T.; Haraguchi, S.; Tamaru, S.-I.; Shinkai, S. *Chem. Asian J.* **2011**, *6*, 266.

(7) (a) Ono, Y.; Nakashima, K.; Sano, M.; Hojo, J.; Shinkai, S. *J. Mater. Chem.* **2001**, *11*, 2419. (b) Photoresponsive organogel based on azobenzene: Zhou, Y.; Xu, M.; Wu, J.; Yi, T.; Han, J.; Xiao, S.; Li, F.; Huang, C. *J. Phys. Org. Chem.* **2008**, *21*, 338. (c) Chen, D.; Liu, H.; Kobayashi, T.; Yu, H. *J. Mater. Chem.* **2010**, *20*, 3610. (d) Lucas, L. N.; Esch, J.; Kellogg, R. M.; Feringa, B. L. *Chem. Commun.* **2001**, 759. (e) Stimuli-responsive gels: Yang, X.; Zhanga, G.; Zhang, D. *J. Mater. Chem.* **2012**, *22*, 38. (f) Cholesterol-based azobenzene switch: Murata, K.; Aoki, M.; Suzuki, T.; Harada, T.; Kawabata, H.; Komori, T.; Ohseto, F.; Keiko, K.; Shinkai, S. *J. Am. Chem. Soc.* **1994**, *116*, 6664. (g) Ajayaghosh, A.; Varghese, R.; George, S. J.; Vijayakumar, C. *Angew. Chem., Int. Ed.* **2006**, *45*, 1141. (h) Ajayaghosh, A.; Praveen, V. K. *Acc. Chem. Res.* **2007**, *40*, 644. (i) de Jong, J. J. D.; Lucas, L. N.; Kellogg, R. M.; van Esch, J. H.; Feringa, B. L. *Science* **2004**, *304*, 278. (j) Azobenzene-based chiral bis(urea) switch: de Loos, M.; van Esch, J.; Kellogg, R. M.; Feringa, B. L. *Angew. Chem., Int. Ed.* **2001**, *40*, 613.

(8) (a) Pijper, D.; Jongejan, M. G. M.; Meetsma, A.; Feringa, B. L. *J. Am. Chem. Soc.* **2008**, *130*, 4541. (b) Pijper, D.; Feringa, B. L. *Soft Matter* **2008**, *4*, 1349.

(9) (a) Chen, C. T.; Chou, Y. C. *J. Am. Chem. Soc.* **2000**, *122*, 7662. (b) Chen, C. T.; Chen, W. C.; Lee, Y. W. *Org. Lett.* **2010**, *12*, 1472. (c) Chen, W. C.; Lin, P. C.; Chen, C. H.; Chen, C. T. *Chem.—Eur. J.* **2010**, *16*, 12822.

(10) (a) Mukhopadhyay, P.; Iwashita, Y.; Shirakawa, M.; Kawano, S. I.; Fujita, N.; Shinkai, S. *Angew. Chem., Int. Ed.* **2006**, *45*, 1592. (b) Hafkamp, R. J. H.; Kokke, B. P. A.; Danke, I. M.; Geurts, M. P. H.; Rowan, A. E.; Feiters, M. C.; Nolte, R. J. M. *Chem. Commun.* **1997**, 545. (c) Helmich, F.; Lee, C. C.; Schenning, A. P. H. J.; Meijer, E. W. *J. Am. Chem. Soc.* **2010**, *132*, 16753. (d) Beginn, U.; Zipp, G.; Mourran, A.; Walther, P.; Möller, M. *Adv. Mater.* **2000**, *12*, 513. (e) Review of dynamic helical structures: Maeda, K.; Yashima, E. *Top. Curr. Chem.* **2006**, *265*, 47. (f) Pratihar, P.; Ghosh, S.; Stepanenko, V.; Patwardhan, S.; Grozema, F. C.; Siebbeles, L. D. A.; Würthner, F. *Beilstein J. Org. Chem.* **2010**, *6*, 1070. (g) Kaiser, T. E.; Stepanenko, V.; Würthner, F. *J. Am. Chem. Soc.* **2009**, *131*, 6719. (h) Würthner, F.; Bauer, C.; Stepanenko, V.; Yagai, S. *Adv. Mater.* **2008**, *20*, 1695. (i) Li, X.-Q.; Zhang, X.; Ghosh, S.; Würthner, F. *Chem.—Eur. J.* **2008**, *14*, 8074. (j) Stilbene as a photoresponsive unit in organogels: Miljanić, S.; Frkanec, L.; Meić, Z.; Žinić, M. *Eur. J. Org. Chem.* **2006**, 1323. (k) Engelkamp, H.; Middelbeek, S.; Nolte, R. J. M. *Science* **1999**, *284*, 785.

(11) See the Supporting Information for the synthesis of **1** and the X-ray crystal structure of its precursor (10*R*,11*R*,*M*)-**11** (Figure S1).